High-Dose Radioimmunotherapy with ^{90}Y-Ibritumomab Tiuxetan: Comparative Dosimetric Study for Tailored Treatment

Marta Cremonesi[1], Mahila Ferrari[1], Chiara Maria Grana[2], Anna Vanazzi[3], Mike Stabin[4], Mirco Bartolomei[2], Stefano Papi[2], Gennaro Prisco[2], Giovanni Martinelli[3], Giovanni Paganelli[2], and Pier Francesco Ferrucci[5]

[1]Division of Medical Physics, European Institute of Oncology, Milan, Italy; [2]Division of Nuclear Medicine, European Institute of Oncology, Milan, Italy; [3]Division of Hematoncology, European Institute of Oncology, Milan, Italy; [4]Department of Radiology and Radiological Sciences, Vanderbilt University, Nashville, Tennessee; and [5]Melanomas and Sarcomas Division, European Institute of Oncology, Milan, Italy

High-dose ^{90}Y-ibritumomab tiuxetan therapy and associated autologous stem cell transplantation (ASCT) were applied after dosimetry. This paper reports dosimetric findings for 3 different methods, including image corrections and actual organ mass corrections. Our first goal was to identify the most reliable and feasible dosimetric method to be adopted in high-dose therapy with ^{90}Y-ibritumomab tiuxetan. The second goal was to verify the safety of the prescribed activity and the best timing of stem cell reinfusion. **Methods:** Twenty-two patients with refractory non-Hodgkin's lymphoma were enrolled into 3 activity groups escalating to 55.5 MBq/kg. A somewhat arbitrary cutoff of 20 Gy to organs (except red marrow) was defined as a safe limit for patient recruitment. ASCT was considered of low risk when the dose to reinfused stem cells was less than 50 mGy. ^{111}In-Ibritumomab tiuxetan (185 MBq) was administered for dosimetry. Blood samples were collected up to 130 h after injection to derive individual blood clearance rates and red marrow doses. Five whole-body images were acquired up to 7 d after injection. A transmission scan and a low-dose CT scan were also acquired. The conjugate-view technique was used, and images were corrected for background, scatter, and attenuation. Absorbed doses were calculated using the OLINDA/EXM software, adjusting doses for individual organ masses. The biodistribution data were analyzed for dosimetry by the conjugate-view technique using 3 methods. Method A was a patient-specific method applying background, scatter, and attenuation correction, with absorbed doses calculated using the OLINDA/EXM software and doses adjusted for individual organ masses and individually estimated blood volumes. Method B was a reference method using the organ masses of the reference man and woman phantoms. Method C was a simplified method using standard blood and red marrow volumes and no corrections. **Results:** The medians and ranges (in parentheses) for dose estimates (mGy/MBq) according to method A were 1.7 (0.3–3.5) for lungs, 2.8 (1.8–10.6) for liver, 1.7 (0.6–3.8) for kidneys, 1.9 (0.8–5.0) for spleen, 0.8 (0.4–1.0) for red marrow, and 2.8 (1.3–4.7) for testes. None of patients had to postpone ASCT. Absorbed doses from method B differed from method A by up to 100% for liver, 80% for kidneys, 335% for spleen, and 80% for blood because of differences between standard and actual masses. Compared with method A, method C led to dose overestimates of up to 4-fold for lungs, 2-fold for liver, 5-fold for kidneys, 7-fold for spleen, 2-fold for red marrow, and 2-fold for testes. **Conclusion:** Patient-specific dosimetry with image correction and mass adjustment is recommended in high-dose ^{90}Y-ibritumomab tiuxetan therapy, for which liver is the dose-limiting organ. Overly simplified dosimetry may provide inaccurate information on the dose to critical organs, the recommended values of administered activity, and the timing of ASCT.

Key Words: high-dose Zevalin; patient-specific dosimetry; autologous stem cell transplantation; NHL; radioimmunotherapy

J Nucl Med 2007; 48:1871–1879
DOI: 10.2967/jnumed.107.044016

Radioimmunotherapy with ^{90}Y-ibritumomab tiuxetan (Zevalin) has shown promising results in phase I–III studies for the treatment of low-grade follicular and high-grade non-Hodgkin's lymphoma, providing statistically and clinically significant higher overall response rates and complete responses than those obtained with rituximab alone, with only transient hematologic toxicity. The potential of this therapy could be further improved if the major limitation of possible severe bone marrow toxicity could be overcome (*1–3*). Red marrow transplantation with associated high-dose ^{90}Y-ibritumomab tiuxetan therapy may be applied, similar to the strategy used in high-dose chemotherapy. In our center, a phase I–II trial based on high-dose ^{90}Y-ibritumomab tiuxetan followed by autologous stem cell transplantation (ASCT) was designed and addressed to patients with refractory or nonresponsive non-Hodgkin's lymphoma. In this study, red marrow toxicity could be surmounted, but critical organs other than red marrow emerged because of higher injected activities. Along with the improved complexity of the

Received Jun. 8, 2007; revision accepted Aug. 18, 2007.
For correspondence or reprints contact: Giovanni Paganelli, MD, Division of Nuclear Medicine, European Institute of Oncology, via Ripamonti, 435, 20141 Milan, Italy.
E-mail: direzione.mnu@ieo.it

therapy, accurate dosimetry information was considered essential in designing the clinical protocol.

An overview of the literature clearly shows that dosimetric results in different centers may not be uniform or comparable (*4*). Dose estimates are often obtained by different methods, with and without various important image corrections, and sometimes using unspecified procedures. The patient-to-patient variability in absorbed doses is frequently difficult to evaluate.

The first dosimetric data on patients treated with ^{90}Y-ibritumomab tiuxetan were obtained from multicenter trials performed to obtain approval from the Food and Drug Administration (*5–7*). These trials found that spleen and liver are the main source organs, red marrow is the critical organ for dosimetry, and activity retention in the body is persistent. Ensuing studies (*8*) focused on obtaining more accurate radiation dose estimates. Additional source organs were identified, and some dose estimates were revised (e.g., the dose to testes was substantially reduced, as it was previously overestimated because of inadequate attenuation correction). In any case, no correlation was found between red marrow dose and toxicity effects (*9*), although the administration of 14.8 MBq/kg has been proved to limit hematologic toxicity. Because red marrow is thought to be the only limiting organ, dosimetry is not required by the U.S. Food and Drug Administration for the standard-protocol use of ^{90}Y-ibritumomab tiuxetan.

However, for high-dose ^{90}Y-ibritumomab tiuxetan associated with ASCT, it was not possible to identify either a "safe" maximal activity to be administered or a unique critical organ for all patients (*10–12*). It was decided that better patient-specific dosimetric information was needed.

This paper reports our dosimetric findings for 3 different methods: method A, patient-specific dosimetry including image corrections for background, attenuation, scatter, and actual organ masses; method B, dosimetry including image corrections but standard organ masses; and method C, simplified dosimetry with standard organ masses and no image corrections.

The principal aim was to evaluate differences between the dosimetric results of the 3 methods and to verify if more simplified methods could to be adopted in the planning of high-dose ^{90}Y-ibritumomab tiuxetan therapy. Identification of the second critical organ with bone marrow rescue was a second endpoint, and finally, the best timing for ASCT after high-dose ^{90}Y-ibritumomab tiuxetan was also investigated.

MATERIALS AND METHODS

Patient Inclusion Criteria

All patients had histologically confirmed refractory or transformed CD20-positive B-cell non-Hodgkin's lymphoma, not suitable for high-dose chemotherapy with ASCT. All patients were older than 18 y; had adequate cardiac, pulmonary, renal, and liver functions; and were negative for bone marrow involvement at the moment of therapy (ascertained by biopsy). Platelets needed to be at least 100×10^9/L, but no limit was fixed for white blood cells and hemoglobin because of the subsequent autologous stem cell reinfusion.

Patient Exclusion Criteria

Pregnancy and lactation were considered exclusion criteria. Patients were also excluded if they had received cytotoxic chemotherapy, external-beam radiotherapy, or cytokine therapy within the previous 4 wk; if they had received prior radioimmunotherapy; or if they had a history of receiving human antimurine antibodies or human antichimeric antibodies. Previous high-dose chemotherapy with ASCT, bulky disease, and prior exposure to rituximab were not considered exclusion criteria.

Patient Study Design

Twenty-two patients (17 men, 5 women; aged 28–75 y) were enrolled into 3 groups of escalating activity. Group I comprised 4 patients who received an activity of 29.6 MBq/kg. The eligibility and allocation of patients to a group receiving a higher activity (group II, 44.4 MBq/kg; or group III, 55.5 MBq/kg) was established on the basis of the dosimetric results. Except for red marrow, the cutoff of 20 Gy to normal organs was considered safe (*13*), and possible higher doses to the spleen were not considered an exclusion criterion (*14*).

Autologous stem cells were collected via apheresis after mobilization with granulocyte colony-stimulating factor alone or together with chemotherapy (cyclophosphamide, 2 g/m^2), having a target of at least 2.0×10^9 CD34+/kg.

The study was approved by the institutional review board of the center, and written informed consent was obtained from all patients.

Radiolabeling

^{111}In-Ibritumomab tiuxetan was radiolabeled according to the manufacturer instructions. An optimized procedure was used to radiolabel the high-activity ^{90}Y-conjugate, as described elsewhere (*15*). At the end of incubation, the reaction was stopped with the provided formulation buffer, containing diethylenetriaminepentaacetic acid to bind any possible free $^{90}Y^{3+}$. The radiochemical purity of ^{111}In-/^{90}Y-ibritumomab tiuxetan was evaluated in triplicate, spotting a small drop on instant thin-layer chromatography silica gel paper, which was subsequently run in saline. The strips were exposed and analyzed in a phosphor-storage-screen radiochromatography scanner (Cyclone; Perkin-Elmer). The radiopharmaceutical was administered only when average radiochemical purity was greater than 98%. The absence of unbound $^{90}Y^{3+}$ and of any additional doses due to its tropism was therefore guaranteed.

Dosimetry

Patients were injected with approximately 185 MBq of ^{111}In-ibritumomab tiuxetan after the infusion of rituximab (250 mg/m^2) for pretreatment dosimetry.

Pharmacokinetics and Biodistribution

Serial blood samples (1 mL) were collected at 15 min; at 1, 3, 5, 16, 24, 48, 90, and 130 h; and on day 7 after injection to determine the individual clearance of antibody from the blood. Before radiopharmaceutical administration, patients underwent a transmission scan using a ^{57}Co-flood source, for possible attenuation correction (*16*), and a low-dose CT scan (80 mA), for evaluation of individual organ masses. Serial scintigraphic whole-body images (anterior and posterior views, 10 cm/min) were acquired at 1, 16, 24, and 48 h and on days 4 and 6 after injection. Energy windows were set at the two ^{111}In peaks (173 and 247 keV, 20%) and at a third interval (140 keV, 9%) for possible scatter correction (*17*). Figure 1 shows

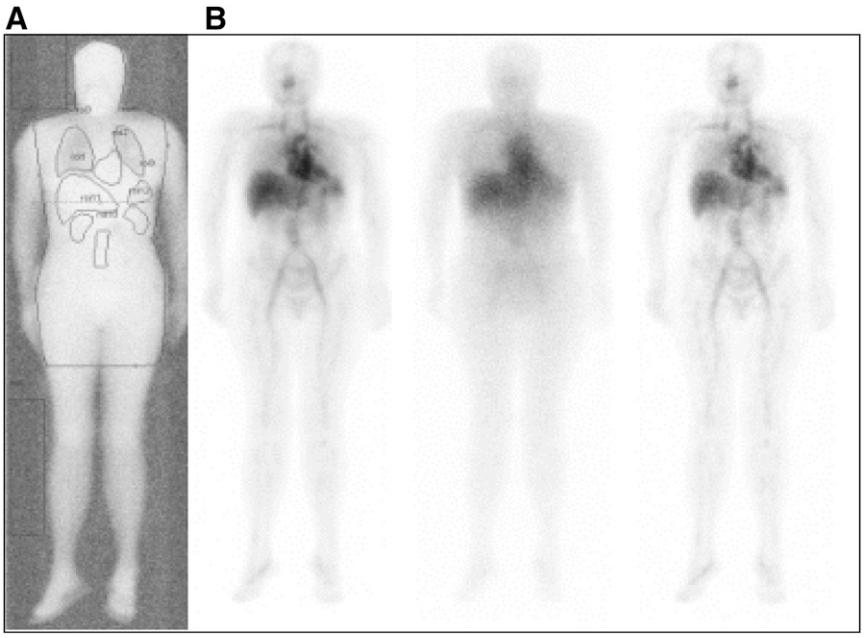

FIGURE 1. Whole-body acquisitions. (A) Transmission scan acquired before injection of radiocompound for possible attenuation correction. Energy window is centered on ^{57}Co peak (122 keV, 20%). Flood source of ^{57}Co was set over 1 of 2 detectors of double-head γ-camera facing patient. (B) From left to right, serial anterior views acquired with energy windows centered on the two ^{111}In peaks (173 and 247 keV, 20%), with energy window centered on 140 keV (9%) for possible scatter correction, and with scatter correction.

the transmission scan, the ^{111}In and scatter window images, and the final scatter-corrected image obtained by image subtraction.

Data Analysis

Three different methods were used for dosimetry evaluation, and the results were analyzed separately.

Method A. The conjugate-view technique was applied to anterior and posterior images after background, scatter, attenuation, and physical decay corrections (*18*). Counts in whole-body images were normalized at the first image, scanning the patient with 100% of the injected activity. The number of decays (NDs) per unit injected activity (*19*)—mathematically equivalent to the previously used quantity of residence time (τ) (*20*)—were calculated from multiexponential fits to the time–activity curves for liver, spleen, lungs, heart wall, kidneys, testes, and remainder of body. The SAAM software (SAAM Institute, University of Washington (*21*)) was used to fit the data using 2 equations:

$$A\%(t) = \sum_i A_i \cdot e^{-a_i \cdot t}$$

for organs with only elimination phases (typically, blood, remainder of body, and lungs) and

$$A\%(t) = A_1 \cdot (1 - e^{-a_1 \cdot t}) + A_2 \cdot (e^{-a_2 \cdot t})$$

for organs with an observable uptake phase in addition to a washout phase (typically, liver, spleen, and testes).

The time–activity curve for blood was evaluated with rescaling for the individual blood mass based on patient sex, weight, and height. The ND in the red marrow (ND_{RM}) was derived from the blood-based method of Sgouros (*22*):

$$ND_{RM} = ND_{blood} \times \frac{m_{RM}}{m_{blood}} \times \left(\frac{0.19}{1 - \text{hematocrit}}\right) = ND_{blood} \times \frac{m_{RM}}{m_{blood}} \times f_o,$$

where m_{RM} and m_{blood} are the individual red marrow and blood masses, hematocrit is the measured patient hematocrit before injection, ND_{blood} is the ND in the blood, and f_0 is 0.19/(1 − hematocrit).

The red marrow mass was derived assuming a fixed ratio of red marrow to blood mass (male, 1,120/5,000; female, 1,300/3,500). The total absorbed dose to red marrow and the dose from 13 d after therapy (due to the ASCT) were extrapolated from the blood curve (Fig. 2). Absorbed doses to target organs were calculated by entering the ND values for all the source organs in the OLINDA/EXM software (*23,24*) and adjusting the doses reported by the software for individual weight and organ masses for kidneys, liver, spleen (determined from CT), and red marrow.

Method B. The influence of mass adjustment on the absorbed dose evaluations was assessed by repeating the calculations for every patient, inserting in OLINDA/EXM the same NDs as in method A but maintaining the organ masses of the reference man and woman phantoms (*19*).

Method C. The time–activity curve for the blood was used to extrapolate ND_{RM} by the blood-derived method, but standard blood and red marrow volumes for male and female subjects were used. The blood clearance curve was fitted by a monoexponential equation. The conjugate view technique was applied to analyze the images, with physical decay correction. The NDs in kidneys, liver, lungs, red marrow, spleen, testes, and remainder of body were calculated by monoexponential fits of the experimental time–activity curves. Reference man and woman organ masses were used for all organs and tissues. Absorbed doses were evaluated with the ZevMIRD spreadsheet (Ryan Belanger Associates (*25,26*)).

For comparison of the results from methods A, B, and C, the ratios of dose for each method were calculated for the target organs of each patient.

Treatment

Twenty of the 22 patients received therapy 1 wk after dosimetry, with the administration of rituximab (250 mg/m^2) followed by the prescribed activity of ^{90}Y-ibritumomab tiuxetan. Although the dosimetry of normal organs was favorable, the clinical evaluation and rapid progression of the disease led to the medical decision to avoid therapy in 2 patients.

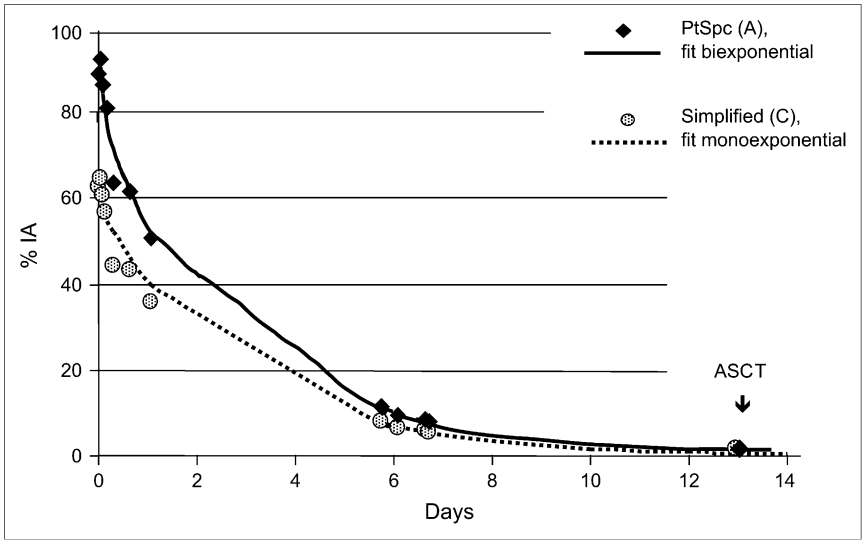

FIGURE 2. Clearance from blood. Time–activity curve for bloodstream of patient evaluated using method A with biexponential fit and using method C with standard blood mass and monoexponential fit. % IA = percentage injected activity; PtSpc = patient-specific.

On the basis of ^{90}Y-ibritumomab tiuxetan blood clearance, ASCT was done 13 d after therapy, unless the estimated dose to the reinfused stem cells suggested that the procedure be delayed for a suitable time (1 or 2 d), to give less than 50 mGy (*14*).

During treatment, adverse events were assessed according to the Common Toxicities Criteria (version 3.0) of the National Cancer Institute.

RESULTS

Masses

For each patient, the actual masses of kidneys, liver, and spleen, assessed by CT, were 306–524 g in men and 281–422 g in women, 1,340–2,330 g in men and 1,060–2,830 g in women, and 183–803 g in men and 90–653 g in women, respectively. The blood volume range was 4,000–6,300 mL in men and 3,260–5,000 mL in women, leading to a red marrow range of 895–1,410 g in men and 1,210–1,855 g in women. The total body weight range was 55–108 kg in men and 58–130 kg in women.

Pharmacokinetics

Clearance from the blood was slow, as expected, with a typical mono- or biexponential trend and a median effective blood half-life of 31.6 h (range, 18.8–66.6 h) with a monoexponential function. Using method A, the median value of ND_{blood} was 38.5 h (range, 18.6–49.8 h), whereas ND_{blood} was approximately 42.8 h (range, 20.0–98.4 h) using method C.

Figure 2 shows 2 different biologic time–activity curves for blood in a female patient: one for the patient-specific blood volume (4,950 mL) and another for the reference woman blood volume (3,500 mL). The experimental data of percentage injected activity in the blood derived with the 2 different hypotheses were fitted by a biexponential function (method A) and a monoexponential function (method C). In this patient, the ND and red marrow absorbed dose were, respectively, 1.89 h and 0.38 mGy/MBq with method A and 2.38 h and 0.84 mGy/MBq with method C, leading to a 120% difference in red marrow dose.

Biodistribution

Figure 3 shows the typical biodistribution in anterior and posterior views. Liver and spleen were the principal source organs. Uptake in kidneys was low, although not negligible, in most patients. Uptake in testes was persistent on late images. Uptake in the lumbar vertebrae was evident in almost all patients.

Absorbed Doses

Dose estimates per unit activity (mGy/MBq) for the 3 methods are reported in Table 1. Using patient-specific evaluations, the median dose to red marrow was 0.83 mGy/MBq (range, 0.38–0.95 mGy/MBq), with the red marrow dose after day 13 always being less than 20% of the total red marrow dose. Taking into account the activities administered to patients, the dose to the reinfused stem cells was always less than 50 mGy, with a median dose of approximately 5 mGy (range, <1–45 mGy).

Table 2 reports the absorbed doses (Gy) estimated by the 3 different methods in the 14 patients allocated to group III (55 MBq/kg).

Figure 4 compares the results for methods A, B, and C using interpatient absorbed dose ratios. Median values and ranges of variability for the target organs of each patient are shown. The impact of mass adjustment on the dose evaluation is shown in reference to the actual organ mass ratio (Fig. 4, dotted bar). Changes in spleen mass most frequently affected the calculations (dose differed by up to 335% when patient-specific and reference-mass results were compared), because of the common association of splenomegaly with the disease.

Even more relevant differences from method A were obtained when absorbed doses assessed using method C

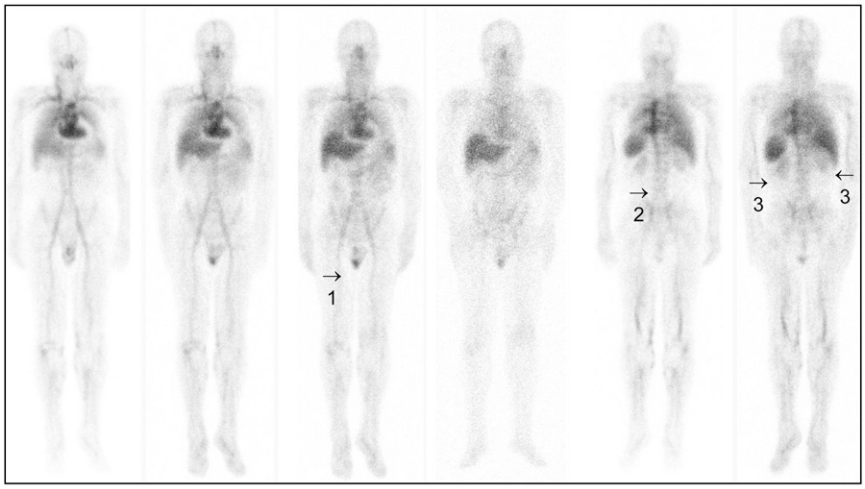

FIGURE 3. Biodistribution images with ^{111}In-ibritumomab tiuxetan. Anterior (ant) and posterior (post) whole-body scintigraphic images (scatter-corrected) were obtained at 2, 18, 80, and 135 h after injection. Images show, in particular, uptake in testes persisting over time (1), bone marrow uptake at level of lumbar vertebrae (2), partially overlapping blood vessel activity in arteries well evident on anterior scans, and nonnegligible uptake in kidneys (3).

where considered (Table 1). Looking at the dose ratios for method C to method A (Fig. 4, black bar), method C caused overestimates of up to 5.1-fold in kidneys (with special influence due to mass adjustment, curve fitting, and background subtraction), 2.0-fold in liver (mass adjustment, curve fitting, and background), 7.1-fold in spleen (mass adjustment, curve fitting, and background), 2.2-fold in red marrow (blood volume adjustment and curve fitting), 4.4-fold in lungs (attenuation), and 2.1-fold in testes (attenuation and curve fitting).

Clinical Impact

Patient recruitment to the 3 therapeutic activity groups was based on method A. The ranges of injected activity were 1.85–2.18 GBq for group I (4 patients), 2.80–3.82 GBq for group II (4 patients), and 3.05–5.55 GBq for group III (14 patients). According to the dosimetric evaluations, 2 patients should have been moved in a lower-level group (1 patient from group II and 1 patient from group III) to avoid giving a liver dose of more than 20 Gy. However, an exception was made for special clinical reasons. The patient in group II, who received a dose of 31 Gy to the liver, went in progression without allowing collection of data for toxicity, whereas no liver toxicity developed in the patient in group III, who received a dose of 25 Gy to the liver.

None of the patients received a dose of more than 10 Gy to lungs, more than 13 Gy to kidneys, or more than 16 Gy to spleen. The dose to kidneys was usually less than 10 Gy, except in 4 patients, who received a dose of between 11 and 13 Gy. Eight of the 22 patients received a dose to red marrow of between 3.1 and 3.8 Gy (7 patients in group III and 1 patient in group II); only 2 patients received more than 4 Gy to red marrow (4.1 and 4.8 Gy), both in group III. Interestingly, the dose to the reinfused stem cells (i.e., the dose to red marrow from day 13 on) never exceeded 50 mGy, and consequently, none of the patients had to delay the PBSC reinfusion schedule. Red marrow fully recovered after stem cell reinfusion, including those cases exceeding 3 and 4 Gy to red marrow.

Conversely, method B would indicate the need to lower the activity in 3 patients to avoid the limit dose to liver. The dose evaluation would exceed 20 Gy to spleen in 5 patients and 3 Gy to red marrow in 11 patients (range, 3.1–5.8 Gy), 6 of whom had doses of more than 4 Gy.

Finally, dosimetric evaluations based on method C would prescribe the shifting of 8 patients in a lower group because of kidney (3 patients), lung (3 patients), or liver (2 patients) doses exceeding the limits established. Moreover, 12 patients would be identified as having doses of more than 20 Gy to spleen and 21 patients as having doses of between 3 and 5 Gy to red marrow (4 of whom had doses of more than 4 Gy). ASCT would be postponed in 2 patients (Table 2,

TABLE 1
Absorbed Doses per Unit Activity to Target Organs Evaluated Using the 3 Methods

Target organ	Absorbed dose		
	Method A	Method B	Method C
Heart wall	2.1 (1.1–5.4)	2.2 (1.0–5.4)	NE
Lungs	1.7 (0.3–3.5)	1.7 (0.4–3.5)	3.2 (0.8–5.1)
Liver	2.8 (1.8–10.6)	3.0 (1.6–8.0)	2.5 (2.1–8.3)
Spleen	1.9 (0.8–5.0)	3.9 (2.4–7.4)	6.1 (3.1–10.2)
Kidneys	1.7 (0.6–3.8)	2.3 (0.9–5.0)	4.0 (2.3–8.1)
Red marrow	0.8 (0.4–1.0)	0.8 (0.5–1.0)	0.8 (0.5–1.6)
Testes (17 patients)	2.8 (1.3–4.7)	2.8 (1.3–4.7)	4.7 (2.5–9.8)
Other organs	0.4 (0.3–0.6)	0.4 (0.3–0.6)	0.5 (0.4–0.6)
Total body	0.5 (0.4–0.8)	0.6 (0.5–0.8)	0.6 (0.5–0.8)

NE = not evaluable.

Data are median values and ranges of variability (mGy/MBq) among patients (4 patients of group I, 4 patients of group II, and 14 patients of group III).

TABLE 2
Absorbed Doses to Principal Target Organs Evaluated Using the 3 Methods

Target organ	Absorbed dose			Clinical impact/notes
	Method A	Method B	Method C	
Lungs	6.1 (1.0–9.7)	6.1 (1.2–9.7)	11.3 (2.4–21.0)	1 C patient exceeding 20 Gy
Liver	11.2 (5.1–31.0)	10.7 (4.4–23.4)	10.6 (5.0–24.2)	2 A patients, 3 B patients, and 2 C patients exceeding 20 Gy
Spleen	6.9 (2.1–15.8)	14.4 (6.0–27.4)	22.1 (9.1–37.1)	5 B patients and 12 C patients exceeding 20 Gy
Kidneys	6.5 (1.1–13.2)	8.1 (1.6–16.8)	14.2 (5.4–23.7)	3 C patients exceeding 20 Gy
Red marrow	2.9 (0.9–4.8)	3.0 (0.9–5.8)	3.5 (1.0–4.9)	2 A patients, 6 B patients, and 4 C patients exceeding 4 Gy
Reinfused stem cells	5.0 ($<$1–45) $\times 10^{-3}$	NE	3.7 ($<$1–130) $\times 10^{-3}$	2 C patients exceeding 50 mGy
Testes	10.1 (2.4–26.3)	10.1 (2.4–26.3)	17.5 (4.6–54.5)	
Total body	2.2 (1.0–2.5)	2.3 (0.9–3.5)	2.6 (1.1–4.3)	

NE = not evaluable.
Data are median values and ranges of variability (Gy) among patients (4 patients of group I, 4 patients of group II, and 14 patients of group III).

last column) because of a dose of more than 50 mGy to the reinfused stem cells.

DISCUSSION

Three major points emerged from this study, the first of these being that the liver was the critical organ for high-dose ^{90}Y-ibritumomab tiuxetan treatment, in contrast to standard ^{90}Y-ibritumomab tiuxetan treatment, because of marrow rescue using ASCT. This point was confirmed by patient-specific dosimetry in all 22 patients. Use of method C would provide misleading information, because kidneys or lungs, rather than liver, would have been identified as the critical organ in 4 patients.

The second major point is that high-dose radioimmunotherapy with ^{90}Y-ibritumomab tiuxetan must be personalized, with patient-specific dosimetry being the method of choice. Several sources of inaccuracies are well known in internal dosimetry, resulting in consistent deviations from the best estimates of dose. In radionuclide targeted therapy, especially with hazardous protocols, it is important to reduce as many causes of uncertainty as possible. A few

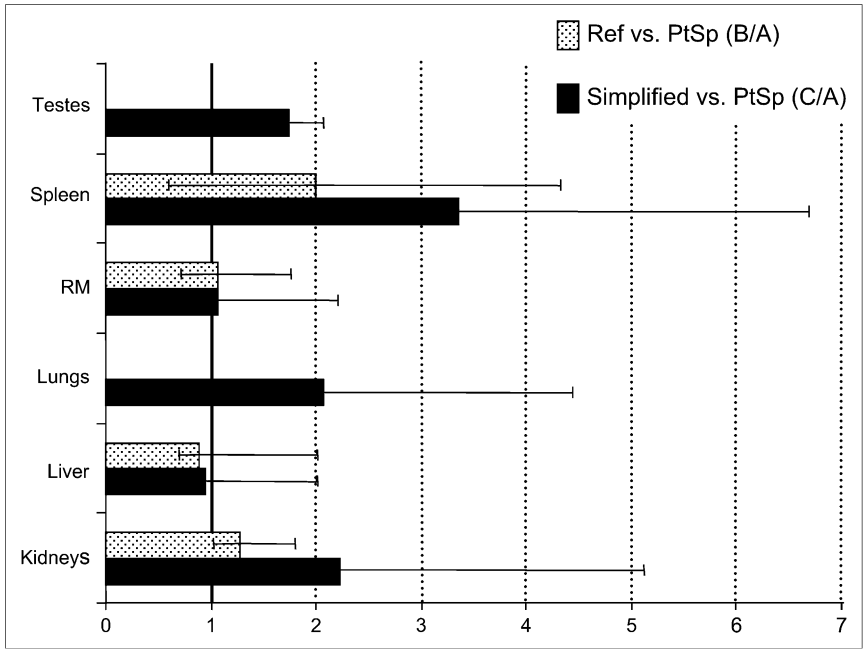

FIGURE 4. Absorbed dose ratios comparing method A with methods B and C. Data are median values and ranges in normal organs. Dotted bar indicates variability in patient-specific/reference-mass dose ratio, with both patient-specific absorbed doses and reference-mass absorbed doses obtained using corrected images and OLINDA/EXM code including or excluding mass adjustment option. Black bar indicates variability in ratio of method A to method C, with patient-specific absorbed doses obtained using OLINDA/EXM code with actual mass adjustments and corrected images. Simplified absorbed doses were obtained using noncorrected images and ZevMIRD code (*25*) with reference phantom (male and female) masses. PtSpc = patient-specific; Ref = reference mass.

comparisons showed that standard organ masses often are not correct for patients affected by serious diseases; actual organ masses should be measured and used whenever possible (*11,12*). Moreover, image correction, especially of attenuation, is necessary to reduce the drawbacks of planar quantification methods; background and scatter corrections may further improve the activity estimates.

The third major point emerging from this study is that accurate evaluation of the time–activity blood curve of each patient allows determination of the timing for ASCT. Because ASCT was planned, the limit of 3 Gy to red marrow for standard ^{90}Y-ibritumomab tiuxetan was not applied. The major focus instead was on delivering minimal irradiation to reinfused stem cells. Again, mass adjustment, but also better regression analyses, avoided nonnegligible overestimates of red marrow doses and the consequent delay of ASCT.

We are aware that transferring an experimental protocol to the clinical setting would require a reasonably easy method, striking a balance between the accuracy and the difficulty of procedures. In routine practice, a simplified procedure is often applied to evaluate dosimetry and delineate the essential dosimetric characteristics of new radiocompounds (*7,25,27*), including standard ^{90}Y-ibritumomab tiuxetan (*25*). However, as the patient-specific vs. simplified dose ratios show (Fig. 4, black bar), an overly simplified method should be avoided because of the clinical impact on tailored high-dose ^{90}Y-ibritumomab tiuxetan therapy (*10–12*). The reported dose estimate results are expected not to be absolutely accurate but certainly more accurate than estimates obtained by the other methods. The assumptions made in the method chosen are more realistic and amply demonstrated in the literature. Certainly, more sophisticated corrections could further refine the dosimetric evaluations, including such corrections as partial background subtraction and compartmental modeling (*18*), but unacceptable discrepancies between more reliable and more simplified evaluations have been shown. The differences imputable to actual mass scaling are considerable but not exhaustive (Fig. 4, dotted bar). Attenuation plays a crucial role, especially for source organs attenuated differently from abdomen (e.g., lungs, testes). Background and scatter also contribute to data uncertainty, and corrections for these effects should be included. It was difficult to summarize the effect of each correction, because the importance and magnitude of each correction varied strongly among patients. This variation was evident in mass adjustment but applied also to attenuation, scatter, and background corrections. However, the importance of any one correction was found to depend on the source organs involved. To summarize, mass adjustment is crucial to avoid over- or underestimation of dose (Fig. 2), especially for spleen, liver, and kidneys; the contribution ranges from negligible to strong and is not always linearly related to the patient's weight. Attenuation correction is of major impact for all organs, especially lungs and testes (e.g., a factor of $\sim$2 in lungs and a factor of in $\sim$3 in testes), and the use of a mean attenuation factor is not appropriate for all organs. Usually, background and scatter corrections are next in importance. If no scatter windows can be set to acquire images, background might include taking into account scatter subtraction, although a specific scatter subtraction is preferable. Finally, the effect of appropriate fitting is lower but still significant: Multiexponential functions typically improved the fits for the time–activity curve of liver and, in some cases, of blood and red marrow. Overall, significant overestimates were observed, up to about 2-fold in liver and red marrow, 2-fold in testes (*28*), 4-fold in lungs, 5-fold in kidneys, and 7-fold in spleen.

The results from method A led to the observation that, following red marrow, liver is the limiting organ. The uptake in kidneys is persistent and nonnegligible in most patients (Fig. 3), particularly in those with compromised renal function. The dose to lungs is usually well below 20 Gy, considered an approximate tolerance dose for lungs in external-beam radiotherapy (the tolerance dose that will produce 5% complications in 5 y [$TD_{5/5}$] is 18 Gy (*29*)). Despite the typically observed high uptake, the dose to spleen was lower than expected, because of the splenomegaly that was present in almost all patients and is often a characteristic of the disease. The dose to ovaries is usually not of concern, but the dose to testes can exceed the threshold of 6 Gy for permanent sterility (*30*), possibly because of the high tissue vascularization. However, sperm cells were recruited from all young patients before they started chemotherapy.

Our median absorbed doses agree with results in the literature except for liver, spleen, and kidneys (heart wall, 2.80 mGy/MBq; lungs, 2.05 mGy/MBq; red marrow, 0.59 mGy/MBq; testes, 2.80 mGy/MBq; total body, 0.54 mGy/MBq; liver, 4.32 mGy/MBq; spleen, 7.35 mGy/MBq; kidneys, 0.22 mGy/MBq) (*8,13,18,28,31,32*). These exceptions can be explained by taking into account the fact that in the previous studies, a whole-body–averaged attenuation correction factor was used instead of a transmission scan for attenuation correction, and kidneys were not identified as major source organs. The number of patients included in the studies (179 vs. 22) was also quite different (*13*), and a comparison of the median values may be of poor value. Moreover, the clinical history of our patients was consistent with a major influence of mass scaling, possibly even more than for the patients usually recruited for standard ^{90}Y-ibritumomab tiuxetan therapy, and especially for spleen, liver, and kidneys (Fig. 4, dotted bar). Finally, the selection of curve fitting can further contribute to differences in the biokinetics of liver and spleen, which typically show a prolonged uptake phase not easily interpretable by monoexponential equations.

In the clinical protocol considered in this study, the limit of 20 Gy for irradiation of the liver, as well as of other vital organs, was a conservative choice (*13*). Actually, higher tolerance doses were indicated from experience with external-beam radiotherapy ($TD_{5/5}$ values of 23 Gy for kidneys and 30 Gy for liver) (*29*). Evidence also exists

that tissue tolerance may be higher during radionuclide therapy than during external-beam radiotherapy (*33,34*) because of the difference in dose rates. Nevertheless, the irradiation of vital organs in patients undergoing high-dose ^{90}Y-ibritumomab tiuxetan deserves special caution because of the clinical history of the patients. Previous aggressive therapies may have affected the liver, red marrow, and kidneys. Irradiation after chemotherapy can generate serious and unpredictable effects. This is a further reason that liver, not lungs, may often be the organ of concern. The dose limit must be applied conservatively because of the possible influence of such prior chemotherapy. Other potential strategies are suggested from this point. If high-dose ^{90}Y-ibritumomab tiuxetan could be proposed as a second-line treatment, higher liver thresholds and, consequently, higher activities of ^{90}Y-ibritumomab tiuxetan could be acceptable.

A final comment on the method used for red marrow dosimetry is worthwhile. The recruited patients had negative bone marrow biopsy findings at the moment of therapy. This fact supported the assessment of red marrow dose by the blood method for monoclonal antibodies (*35,36*), which was considered the reference in therapy-planning evaluations. However, in many patients scintigraphic images suggested some bone marrow uptake, especially in the vertebrae, with intensities that did not necessarily vary in relation to the disease. This finding raised the possibility that a contribution from specific marrow uptake could be missed (*37,38*). If so, the absence of a correlation between dose and toxicity, stated in the literature, might be partially explained, and a more adequate model for the red marrow dose should be applied to minimize the chance of toxicity. This topic should be further explored and possibly compared with the toxicity of the ASCT.

CONCLUSION

In high-dose ^{90}Y-ibritumomab tiuxetan therapy, overly simplified dosimetry methods may produce misleading indications, lowering allowable values of administered activity and shifting the time of autologous stem cell reinfusion. We suggest that tailored therapy be performed after patient-individualized dosimetry, with adjustment of standard model organ masses to patient-specific values and with application of all possible image corrections.

With marrow rescue, the liver is the second limiting organ in these cases. Calculation of liver dose deserves special attention because of the large number of chemotherapy lines that the patient population typically receives.

An accurate dosimetric evaluation is mandatory in new clinical trials designed to increase the chances of cure not only in nonresponding patients but also, possibly, in the early stages of therapeutic planning.

ACKNOWLEDGMENTS

We thank Deborah Console for typing the manuscript, and we thank Annalisa Rossi, Dr. Silvia Melania Baio, Dr. Demetrio Aricò, Dr. Liliana Calabrese, and Angela Cocquio for assisting the patients. We are especially grateful to Dr. Jeff Siegel for useful discussions and to the Italian Association for Cancer Research (AIRC) for financial support.

REFERENCES

1. Witzig TE, Gordon LI, Cabanillas F, et al. Randomized controlled trial of yttrium-90–labeled ibritumomab tiuxetan radioimmunotherapy versus rituximab immunotherapy for patients with relapsed or refractory low-grade, follicular, or transformed B-cell non-Hodgkin's lymphoma. *J Clin Oncol.* 2002;20:2453–2463.
2. Witzig TE, Flinn IW, Gordon LI, et al. Treatment with ibritumomab tiuxetan radioimmunotherapy in patients with rituximab-refractory follicular non-Hodgkin's lymphoma. *J Clin Oncol.* 2002;20:3262–3269.
3. Morschhauser F, Illidge T, Huglo D, et al. Efficacy and safety of yttrium 90 ibritumomab tiuxetan in patients with relapsed or refractory diffuse large B-cell lymphoma not appropriate for autologous stem cell transplantation. *Blood.* 2007;110:54–58.
4. Wessels BW, Bolch WE, Bouchet LG, et al. Bone marrow dosimetry using blood-based models for radiolabeled antibody therapy: a multiinstitutional comparison. *J Nucl Med.* 2004;45:1725–1733.
5. Wiseman GA, White CA, Stabin M, et al. Phase I/II ^{90}Y-Zevalin (yttrium-90 ibritumomab tiuxetan, IDEC-Y2B8) radioimmunotherapy dosimetry results in relapsed or refractory non-Hodgkin's lymphoma. *Eur J Nucl Med.* 2000;27:766–777.
6. Zevalin Web site. Zevalin support services page. Available at: http://www.zevalin.com/SupportServices/supportService.htm. Accessed August 30, 2007.
7. U.S. Food and Drug Administration Web site. Review of biologics license application for IDEC pharmaceutical ZEVALIN™ kit, BLA no. 125019. Available at: http://www.fda.gov/ohrms/dockets/ac/01/briefing/3782b2_03_FDA%20Backgrounder.pdf. Accessed August 30, 2007.
8. Wiseman GA, Leigh BR, Dunn WL, Stabin MG, White CA. Additional radiation absorbed dose estimates for Zevalin™ radioimmunotherapy. *Cancer Biother Radiopharm.* 2003;18:253–258.
9. Wiseman GA, Leigh BR, Erwin WD, et al. Radiation dosimetry results from a phase II trial of ibritumomab tiuxetan (Zevalin) radioimmunotherapy for patients with non-Hodgkin's lymphoma and mild thrombocytopenia. *Cancer Biother Radiopharm.* 2003;18:165–178.
10. Siegel JA, Stabin MG, Brill AB. The importance of patient-specific radiation dose calculations for the administration of radionuclides in therapy. *Cell Mol Biol (Noisy-le-grand).* 2002;48:451–459.
11. Cremonesi M, Ferrari M, Stabin M, et al. Comparison of dosimetry methods for high dose Zevalin therapy in refractory NHL patients [abstract]. *J Nucl Med.* 2005;46(suppl):87P.
12. Rajendran JG, Fisher DR, Gopal AK, Durack LD, Press OW, Eary JF. High-dose ^{131}I-tositumomab (anti-CD20) radioimmunotherapy for non-Hodgkin's lymphoma: adjusting radiation absorbed dose to actual organ volumes. *J Nucl Med.* 2004;45:1059–1064.
13. Wiseman GA, Kornmehl E, Leigh B, et al. Radiation dosimetry results and safety correlations from ^{90}Y-ibritumomab tiuxetan radioimmunotherapy for relapsed or refractory non-Hodgkin' lymphoma: combined data from 4 clinical trials. *J Nucl Med.* 2003;44:465–474.
14. Nademanee A, Forman S, Molina A, et al. A phase 1/2 trial of high-dose yttrium-90-ibritumomab tiuxetan in combination with high-dose etoposide and cyclophosphamide followed by autologous stem cell transplantation in patients with poor-risk or relapsed non-Hodgkin lymphoma. *Blood.* 2005;106:2896–2902.
15. Papi S, Urbano N, Tosi G, Ferrari M, Paganelli G, Chinol M. Radiolabeling of Zevalin® with high ^{90}Y activity: optimization of the procedure and reduction of the radiopharmacist radiation exposure [abstract]. *Eur J Nucl Med Mol Imaging.* 2006;33(suppl):S90.
16. Savi A, Lecchi M, Albertini F, et al. Evaluation of attenuation correction in planar In-111 biodistribution studies [abstract]. *Eur J Nucl Med Mol Imaging.* 2004;31(suppl):S229.
17. Cremonesi M, Migliazza M, Bodei L, et al. Reconstruction algorithm validation for In-111-labelled radiopharmaceuticals in hybrid SPECT-CT imaging system [abstract]. *Eur J Nucl Med.* 2002;29(suppl):S93.
18. Siegel JA, Thomas SR, Stubbs JB, et al. Techniques for quantitative radiopharmaceutical biodistribution data acquisition and analysis for use in human radiation dose estimates: MIRD pamphlet no.16. *J Nucl Med.* 1999;40(suppl):S37–S61.
19. Stabin MG, Siegel JA. Physical models and dose factors for use in internal dose assessment. *Health Phys.* 2003;85:294–310.

20. Loevinger R, Budinger TF, Watson EE. *MIRD Primer for Absorbed Dose Calculations.* Reston, VA: Society of Nuclear Medicine; 1988.
21. Foster D, Barret P. Developing and testing integrated multicompartment models to describe a single-input multiple-output study using the SAAM II software system. In: *Proceedings of the Sixth International Radiopharmaceutical Dosimetry Symposium.* Oak Ridge, Tennessee: Oak Ridge Institute for Science and Education;1998.
22. Sgouros G. Bone marrow dosimetry for radioimmunotherapy: theoretical considerations. *J Nucl Med.* 1993;34:689–694.
23. Stabin MG, Sparks RB, Crowe E. OLINDA/EXM: the second-generation personal computer software for internal dose assessment in nuclear medicine. *J Nucl Med.* 2005;46:1023–1027.
24. RADAR Web site. Available at: www.doseinfo-radar.com. Accessed August 30, 2007.
25. Belanger R. *ZevMIRD: A Workbook for Zevalin® Dosimetry.* San Diego, CA: Ryan–Belanger Associates; 1997.
26. Stabin MG. MIRDOSE: Personal computer software for internal dose assessment in nuclear medicine. *J Nucl Med.* 1996;37:538–546.
27. Forster GJ, Engelbach MJ, Brockmann JJ, et al. Preliminary data on biodistribution and dosimetry for therapy planning of somatostatin receptor positive tumours: comparison of ^{86}Y-DOTATOC and ^{111}In-DTPA-octreotide. *Eur J Nucl Med.* 2001;28:1743–1750.
28. Wiseman GA, Leigh BR, Dunn WL, Stabin MG, White CA. Additional radiation absorbed dose estimates for Zevalin™ radioimmunotherapy. *Cancer Biother Radiopharm.* 2003;18:253–258.
29. Emami B, Lyman J, Brown A, et al. Tolerance of normal tissue to therapeutic irradiation. *Int J Radiat Oncol Biol Phys.* 1991;21:109–122.
30. International Commission on Radiological Protection. *Radiological Protection on Biomedical Research: ICRP Publication 62.* New York, NY: Pergamon Press; 1992. ICRP62.
31. Wu RK, Siegel JA. Absolute quantitation of radioactivity using the buildup factor. *Med Phys.* 1984;11:189–192.
32. Tennvall J, Fischer M, Bischof Delaloye A, et al. EANM procedure guideline for radio-immunotherapy for B-cell lymphoma with ^{90}Y-radiolabelled ibritumomab tiuxetan (Zevalin). *Eur J Nucl Med Mol Imaging.* 2007;34:616–622.
33. Barone R, Borson-Chazot F, Valkema R, et al. Patient-specific dosimetry in predicting renal toxicity with ^{90}Y-DOTATOC: relevance of kidney volume and dose rate in finding a dose–effect relationship. *J Nucl Med.* 2005;46(suppl):99S–106S.
34. Dale R, Carabe-Fernandez A. The radiobiology of conventional radiotherapy and its application to radionuclide therapy. *Cancer Biother Radiopharm.* 2005;20:47–51.
35. Sgouros G, Stabin M, Erdi Y, et al. Red marrow dosimetry for radiolabeled antibodies that bind to marrow, bone, or blood components. *Med Phys.* 2000;27: 2150–2164.
36. Sgouros G. Dosimetry of internal emitters. *J Nucl Med.* 2005;46(suppl):18S–27S.
37. Shen S, Meredith RF, Duan J, et al. Improved prediction of myelotoxicity using a patient-specific imaging dose estimate for non-marrow-targeting ^{90}Y-antibody therapy. *J Nucl Med.* 2002;43:1245–1253.
38. Siegel J, Lee R, Pawlyk D, Horowitz J, Sharkey R, Goldenberg D. Sacral scintigraphy for bone marrow dosimetry in radioimmunotherapy. *Int J Appl Radiat Instr* 1989;16:553–559.